Proceedings of the 40th IEEE
Conference on Decision and Control
Orlando, Florida USA, December 2001

Hovering Flight Control of a Micromechanical Flying Insect*

Xinyan Deng, Luca Schenato, Shankar Sastry
Department of Electrical Engineering and Computer Sciences
University of California at Berkeley
{xinyan|lusche|sastry}@robotics.eecs.berkeley.edu

Abstract

This paper describes recent results on the design and simulation of a flight control strategy for the Micromechanical Flying Insect (MFI), a 10-25mm (wingtip-to-wingtip) device capable of sustained autonomous flight. Biologically inspired by the real insect's flight maneuver, the wing kinematics are paremetrized by a small set of parameters which are sufficient to generate desired average torques to regulate its attitude. Position control was achieved through attitude control based on the linearized dynamics under small angle assumption near hovering. During its continuous flight, the controller schedules the desired wing kinematic parameters according to the inverse map based on the feedback error at the end of each wingbeat. The proposed controller was simulated with the Virtual Insect Flight Simulator, and the results show convergence of both position and orientation.

1 Introduction

Unmanned air vehicles, (UAV), have been a very active area of research. Despite recent remarkable achievements obtained with fixed and rotary aircrafts [1] [2], their use in many tasks is still limited by their maneuverability and size. However, the extraordinary flight capabilities of insects have inspired the design of small UAVs with flapping wings mimicking real flying insects. Their unmatched maneuverability, low fabrication cost and small size make them very attractive for cost-critical missions in environments which are unpenetrable for larger size UAVs. Moreover, the latest advances in insect flight aerodynamics and microtechnology seem to provide sufficient tools to fabricate flying insect micro-robots. This is the challenge that the Micromechanical Flying Insect project (MFI) being currently developed at UC Berkeley, has taken [3], [4]. Figure 1 shows a conceptual view of the target robot fly.

Similar to aerial vehicles based on rotary wings, such as helicopter, flying insects control their flight by controlling their attitude and the magnitude of the vertical thrust [5]. This is accomplished by the aerodynamic forces and torques generated from the wing flapping motion. However, different from aerodynamic forces exerted on helicopter blades, aerodynamic forces on insect wings are highly nonlinear and time-varying along a wingbeat, and the periodic motion of the wings cannot be ignored. As a result, the system dynamics cannot be approximated by a linear time-invariant model, as is widely adopted by rotorcrafts based on quasi-static assumption on the rotary blades. The motion of the insect is a complex nonlinear oscillation with forced periodic inputs under non-holonomic constraints. Moreover, the total force and torques on the MFI body are the result of those generated by the two wings. Therefore, techniques like feedback linearization [6] and robust linear control [7] are likely to fail, unless a better understanding of insect flight dynamics is available.

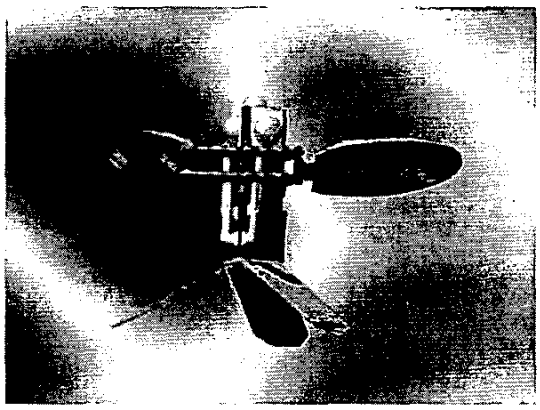

Figure 1: MFI model based on a blow fly calliphora, with a mass of $100\,mg$, wing length of $11\,mm$, wing beat frequency of $150\,Hz$, and actuator power of $10\,mW$. Each of the wing has two degree of freedom: flapping and rotation.

Although very little is known about how real insects accomplish in controlling their flight and maneuver, recent work has found that by modulating a few kinematic parameters on each wing, such as wing rotation timing at the stroke reversals and the wing blade angle of attack, the insect can readily apply torques on the body and therefore control its attitude and position [8]. Based on this observation, it was suggested that a small set of wing kinematics might be sufficient to generate all possible flight modes, and the key point for designing any of these modes is the capability to control the MFI's attitude [5].

This paper describes the design and the implementation

*This work was funded by ONR MURI N00014-98-1-0671, ONR DURIP N00014-99-1-0720 and DARPA.

of a flight control strategy for the MFI. The challenging task of the control of MFI have forced the development of novel approaches and biologically inspired techniques. As a first step, we parameterize the wing kinematics by three parameters which are related to wing flip timing and mean angle of attack during one wingbeat. Then, the map between these parameters and mean torques generated during the wingbeat are found and tested. Based on the weighed position and attitude feedback error, we propose a switching controller which schedules the next wingbeat parameters according to the inverse map. Since position control is obtained under the assumption of small angular displacement, we put more weights on the angular error in order to stabilize the flight.

2 Insect Aerodynamics

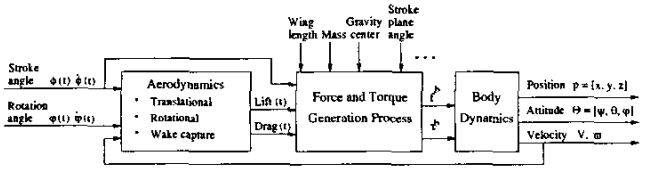

Figure 2: The model for the insect dynamics.

A complete model of an insect can be divided into three different subsystems, which are the *aerodynamics*, *force and torque generation process*, and *body dynamics* as shown in Figure 2. Stroke angles and rotation angles are defined in Figure 3, together with lift and drag aerodynamic forces generated from the flapping of the wings.

As seen from Figure 2, the *actuator dynamics* is ignored, which will be designed as a PWM to drive the stroke and rotation angles into periodic motion. In this paper, it is assumed that the input angles take form of trigonometric functions and their amplitude and phase can be modulated directly.

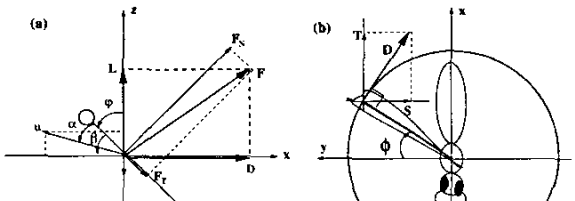

Figure 3: Aerodynamic forces decomposed into lift(L) and drag(D) forces in stroke plane; (a) lateral view; (b) top view; ϕ: stroke angle, φ: rotation angle, α: angle of attack, u: wing velocity.

Although at present no numerical simulation of unsteady insect flight aerodynamics gives exact results for aerodynamic forces, several advances have been achieved in comprehending qualitatively and quantitatively unsteady state aerodynamic mechanism [8]. From our previous work, the aerodynamic module is a combination of an analytical model, based on quasi-steady state equations for the delayed stall and rotational circulation, and an empirically matched model based on Robofly data [9]. It is a highly nonlinear model involving discontinuous functions, time-varying parameters (lift and drag coefficients, C_D, and C_L) and model uncertainties (due to neglect of wake capture).

Given lift, drag forces and stoke angle, the total wrench (forces and torques) in the *stroke plane* can be obtained, proceeded by a *coordinate transformation*, the total wrench in the *body frame* can be derived. As shown in [10], the equations of motion for a rigid body subject to an external wrench $F^b = [f^b, \tau^b]^T$ applied at the center of mass and specified with respect to the body coordinate frame is given by Newton-Euler equations, which can be written as

$$\begin{bmatrix} mI & 0 \\ 0 & \mathcal{I} \end{bmatrix} \begin{bmatrix} \dot{v}^b \\ \dot{\omega}^b \end{bmatrix} + \begin{bmatrix} \omega^b \times mv^b \\ \omega^b \times I\omega^b \end{bmatrix} = \begin{bmatrix} f^b \\ \tau^b \end{bmatrix} \quad (1)$$

where I is the inertia matrix. v^b is the velocity vector of the center of mass in spatial coordinates, and ω^b is the angular velocity vector in body frame. Let R represents the rotation matrix of the body axes relative the the spatial axes, we have $\dot{P} = v^p = Rv^b$ and $\hat{\omega}^b = R^T\dot{R}$.

For $R \in SO(3)$, we parameterize R by ZYX Euler angles with ϕ, θ, and ψ about x,y,z axes respectively, and hence $R = e^{\hat{z}\psi}e^{\hat{y}\theta}e^{\hat{x}\phi}$ with $x = [1\ 0\ 0]^T$, $y = [1\ 0\ 0]^T$,$z = [0\ 0\ 1]^T$ and $\hat{x}, \hat{y}, \hat{z} \in SO(3)$. By differentiating R with respect to time, we have the state equations of the Euler angles, $\Theta = [\phi\ \theta\ \psi]^T$, which can be defined as $\dot{\Theta} = W\omega^b$. By defining the state vector $[P, \Theta] \in R^3 \times R^3$ where P is the position of the center of mass with respect to the inertia frame, and Θ are the Euler angles which we use to parameterize the rotation matrix R, the equations of motion of the insect is written as

$$\begin{aligned} \ddot{P} &= \frac{1}{m}Rf^b \\ \ddot{\Theta} &= (IW)^{-1}[\tau^b - W\dot{\Theta} \times IW\dot{\Theta} - I\dot{W}\dot{\Theta}] \end{aligned} \quad (2)$$

where the body forces and torques are periodic, nonlinear functions of the wing kinematics. *i.e.*

$$\begin{aligned} f^b &= f^b(\phi_i(t), \dot{\phi}_i(t), \varphi_i(t), \dot{\varphi}_i(t)) \\ \tau^b &= \tau^b(\phi_i(t), \dot{\phi}_i(t), \varphi_i(t), \dot{\varphi}_i(t)) \end{aligned} \quad (3)$$

where $i \in \{l, r\}$ represents the left and right wing, respectively.

3 Linearized Insect Dynamics

The dynamics of the insect can be expressed as a nonlinear time-varying MIMO system as in Equations 2 and Equation 3, whose analytical solution is beyond scope of currently existing techniques. As it is pointed out before, the motion of the insect is a complicated nonlinear oscillation with forced periodic inputs under nonholonomic constraints (stroke angle amplitude), therefore current control techniques such as feedback linearization and robust linear control are likely to fail. Another important difficulty for the design of a flight controller arising in practice is the high uncertainty of the aerodynamic model for insect flight. Though the qualitative aspects of the aerodynamics involved are becoming clear and it is possible to safely estimate the mean forces averaged over a whole flapping cycle, no exact quantitative model is available for the instantaneous forces at present. The challenging task of the control of MFI has forced the development of novel approaches and biologically inspired techniques.

As a first approximation, in near hovering condition, where the angles are small, neglecting nonlinearity and coupling among variables, the dynamics of the MFI is given by:

$$\begin{aligned} \ddot{\eta} &= I_{\eta}^{-1}\tau_{\eta}(t) \\ \ddot{\theta} &= I_{\theta}^{-1}\tau_{\theta}(t) \\ \ddot{\psi} &= I_{\psi}^{-1}\tau_{\psi}(t) \\ \ddot{x} &= m^{-1}F_v(t)\sin(\theta) \\ \ddot{y} &= -m^{-1}F_v(t)\sin(\eta) \\ \ddot{z} &= m^{-1}F_v(t) - g \end{aligned} \tag{4}$$

where $[I_{\eta}, I_{\theta}, I_{\psi}]$ are the moment of inertia of the roll, pitch and yaw axes respectively, $[\tau_{\eta}, \tau_{\theta}, \tau_{psi}]$ are the corresponding torques generated by the wings, m is the total mass of the insect, F_v is the mean aerodynamic vertical thrust, and g is the gravitational acceleration.

If the orientation angles of MFI are small, the position dynamics can be simplified as follows:

$$\begin{aligned} x^{(4)} &= m^{-1}I_{\theta}^{-1}F_v(t)\tau_{\theta}(t) \\ y^{(4)} &= -m^{-1}I_{\eta}^{-1}F_v(t)\tau_{\eta}(t) \\ z^{(2)} &= m^{-1}F_v(t) - g \end{aligned} \tag{5}$$

where the index in the parenthesis stands for the order of the derivative. Though this is a very crude approximation, it clearly evidences how position control can be achieved by controlling only three parameters, the roll torque,τ_{η}, the pitch torque, τ_{θ}, and the vertical thrust, F_v.

4 Wing Kinematics Parameterization

Inspired by biological observations, we need to parameterize the wing kinematics to generate desired control torques about the roll, pitch, and yaw axis. Recent work [8] have envidenced two main control mechanism adopted by insects for torque control: *phase of rotation* and *mean angle of attack*. The key idea in this section is to parameterize the wing kinematics such that we can decouple the control of the three torques, thus simplify the design of the hovering controller. A different mean angle of attack and the phase of rotation between the two wings can generate asymmetrical instantaneous forces along a wingbeat, thus giving rise to positive or negative mean torque and forces. Intuitively, the mean angle of attack can modulate the magnitude of the aerodynamic forces on the wing: lift is maximal at an angle of attack of 45^o and decreases for different angles. The advanced or delayed phase of rotation respectively increases or decreases both lift and drag at the stroke reversals.

These findings suggest how to select wing kinematics that generate desired torques. Figure 4 shows *only some* of such kinematics. In the scenario (A) the wings have the same motion stroke angle motion and the phase of wings rotation, $\varphi(t)$, is advanced on the back of the insect body and delayed on the front, giving rise to a net pitch down torque. In the scenario (B) the wings have the same stroke angle motion, $\phi(t)$, but the phase of rotation for the left wing is advanced on the back of the insect body and delayed on the front, and it is opposite on the right wing, giving rise to a net clockwise yaw torque. In the scenario (C) the wings have the same stroke angle motion, $\phi(t)$, and phase of rotation, but the right wing has a smaller mean angle of attack, giving rise to a net right roll torque.

Furthermore, experiments with Robofly [8] showed that the two most important parameters for torque generation are the mean angle of attack and the timing of rotation at the end of each half-stroke. Following these observations, we parameterize the motion of the wings with only three parameters as follows:

$$\begin{aligned} \phi_r(t) &= \phi_l(t) = \Phi\sin(2\pi f t) \\ \varphi_r(t) &= \Upsilon_r\left[\sin(2\pi f t) + \alpha_r\sin(4\pi f t)\right] \\ \varphi_l(t) &= \Upsilon_l\left[\sin(2\pi f t) + \alpha_l\sin(4\pi f t)\right] \\ \Upsilon_l &= \frac{\pi}{4} + \frac{\pi}{8}ramp(\gamma) \\ \Upsilon_r &= \frac{\pi}{4} + \frac{\pi}{8}ramp(-\gamma) \end{aligned} \tag{6}$$

where ϕ is the stroke angle, f is the wingbeat frequency, Φ is the maximal stroke amplitude, φ is the rotation angle, Υ is the maximal rotation angle and the subscript r and l stand for right and left wing, respectively. The function $ramp()$ is defined as follows:

$$ramp(\gamma) = \begin{cases} 0 & : \quad \gamma < 0 \\ \gamma & : \quad \gamma \geq 0 \end{cases} \tag{7}$$

The parameters α_l and α_l are strongly related to wing flip timing: a positive value corresponds to advancing the wing rotation on the downstroke and delaying on the upstroke, a negative value does the opposite,

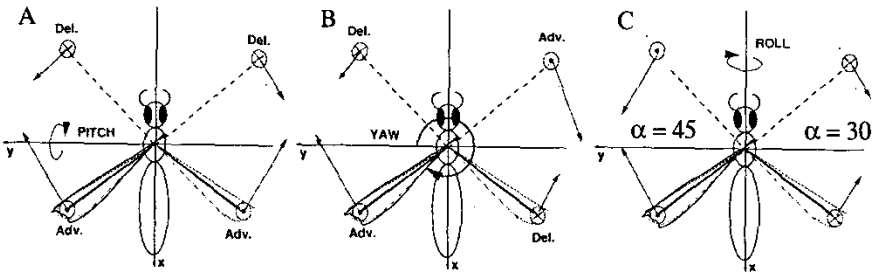

Figure 4: Open loop wing motions that can generate: (A) pitch, (B) yaw, (C) roll torques. The arrows represent the instantaneous aerodynamic forces acting on the wings. The circles with a cross or with a dot correspond, respectively to the perpendicular component of the force entering or exiting the stroke plane. `Adv.` and `Del.` stand for advanced and delayed rotation respectively.

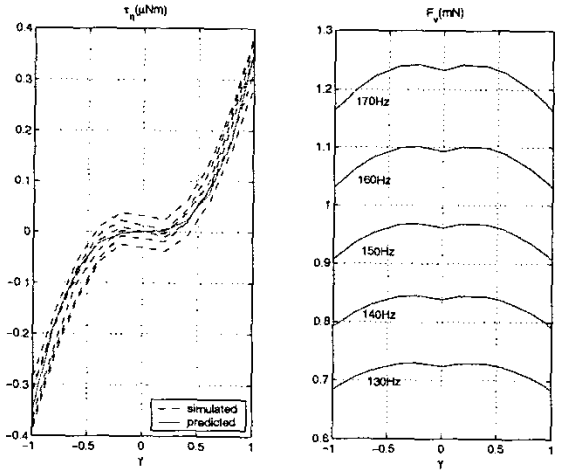

Figure 5: Average roll torque, τ_η, map (left) as a function of the parameter γ and different values for the other two parameters (dotted lines). The solid line corresponds to the approximate function $\tau_\eta = c^{-1}\gamma^3$. Mean lift, f_z, calculated at different frequencies (right).

a null value results in a symmetric wing rotation at both the half-strokes. The parameter γ modifies the mean angle of attack of the wings: a negative value corresponds to a smaller mean angle of attack on the right wing, a positive value to the opposite, and a zero value to equal mean angle of attack. According to this parameterization, scenario (A) is given by, $\gamma = 0$, and $\alpha_r = \alpha_l = 0.4$; scenario (B) is given by,$\gamma = 0$, $\alpha_r = 0.4$ and $\alpha_l = -0.4$;scenario (C) is given by, $\gamma = 2/3$, and $\alpha_r = \alpha_l = 0$.

By varying these three parameters, it is possible to generate sufficient torque to steer the MFI body about the roll, pitch, and yaw axes. In particular, the map from wing kinematics to the average torque over one wingbeat $f() : \mathcal{R}^3_u \rightarrow \mathcal{R}^3_\tau$ can be written as follows:

$$\begin{aligned} \bar{\tau}_\eta &= f_1(\alpha_r, \alpha_l, \gamma) \\ \bar{\tau}_\theta &= f_2(\alpha_r, \alpha_l, \gamma) \end{aligned}$$

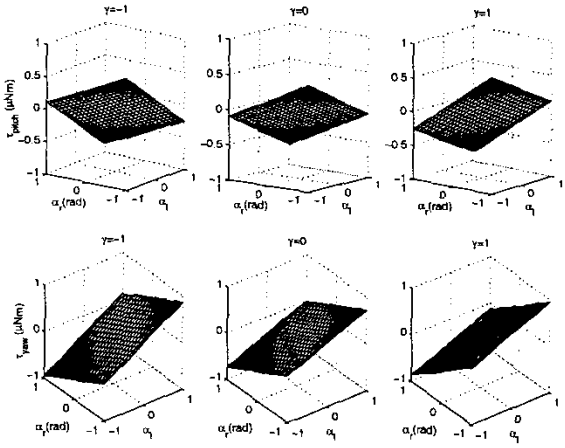

Figure 6: Average pitch and yaw torque maps.

$$\bar{\tau}_\psi = f_3(\alpha_r, \alpha_l, \gamma) \quad (8)$$

In order to change the average vertical thrust to balance the insect's weight, it is sufficient to change the wing flapping frequency. Indeed, simulation results show that by switching between two frequencies (150 ± 10 Hz), it is sufficient to generate average positive or negative vertical forces. Furthermore, torque changes resulting from this frequency change can be neglected.

Figure 5 and Figure 6 show the simulation results obtained from Virtual Insect Flight Simulator (VIFS) with the morphology of a honey bee. Consequently, given the values for the mean torques we want to generate in a wingbeat, the values for the wing parameters α_l, α_r and γ can be obtained from the inverse map, $g() = f^{-1}() : \mathcal{R}^3_\tau \rightarrow \mathcal{R}^3_u$. The function $g()$ does not necessarily exist. It depends on the chosen parameterization of the wings motion and on the velocity of the insect body. However, Figure 5 and 6 show that f_2 and f_3 are approximate linear functions of α_l and α_r only, while f_1 is an approximated function of γ only. Therefore, the inverse map $\hat{g}()$ is approximated as follows:

$$\hat{\gamma} = \hat{g}_1(\bar{\tau}_\eta) = c\,\bar{\tau}_\eta^{\frac{1}{3}}$$

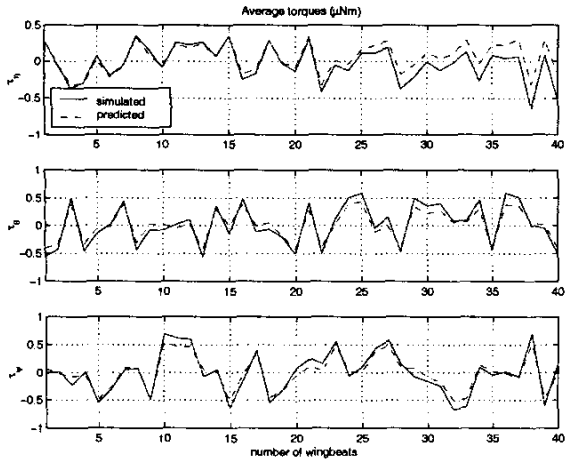

Figure 7: Comparison of the average torques calculated from approximate functions and those from the simulation, over a consequetive 40 wingbeats; γ, α_l, and α_r are chosen randomly.

$$\begin{aligned} \hat{\alpha}_l &= \hat{g}_2(\bar{\tau}_\theta, \bar{\tau}_\psi) = a_{11}\,\bar{\tau}_\theta + a_{12}\,\bar{\tau}_\psi \\ \hat{\alpha}_r &= \hat{g}_3(\bar{\tau}_\theta, \bar{\tau}_\psi) = a_{21}\,\bar{\tau}_\theta + a_{22}\,\bar{\tau}_\psi \end{aligned} \tag{9}$$

where the parameters, $c, a_{11}, a_{12}, a_{21}, a_{22}$ are constant. The function $\hat{g}()$ is a simple function of the mean torques and can be readily inverted. Moreover, the parameter γ is almost decoupled from the yaw and pitch torques.

In order to evaluate the approximation map in a more realistic setting, we simulate the MFI motion in VIFS by randomly choosing the value of the parameters $\gamma, \alpha_l, \alpha_r$ for a consequetively 40 wingbeats. In this setting, coupling factors among the parameters and insect body velocities are taken into account. Figure 7 shows the mean torque predicted by the approximate map $\hat{g}^{-1}()$ and the mean torque per wingbeat actually calculated from the simulation, corresponding to the real map $f()$. It shows that the approximate map matches the real value very well and is very promising in the prospective of designing feedback control.

5 Switching Control Approach

To simplify the analysis we assume perfect state information, i.e. position, attitude and velocity of the MFI are accessible. Based on the crude dynamic model derived in Section , a switching controller is designed. It functions as a scheduler which selects the next wingbeat kinematic parameters, based on the feedback error at the end of current wingbeat.

It should be noted that this is an average controller in the sense that it only changes the inputs at the end of every wingbeats, while the insect is in continuous motion. However, in the case of high frequency when the chattering of the motion is small, the response of the real model can be approximated by an average one. The feedback law is based on average errors calculated at the end of every wingbeat

$$\begin{aligned} \bar{e}_\eta &= -k_{\eta 1}\dot{\bar{\eta}} - k_{\eta 0}\bar{\eta} \\ \bar{e}_\theta &= -k_{\theta 1}\dot{\bar{\theta}} - k_{\theta 0}\bar{\theta} \\ \bar{e}_\psi &= -k_{\psi 1}\dot{\bar{\psi}} - k_{\psi 0}\bar{\psi} \\ \bar{e}_x &= -k_{x3}\bar{x}^{(3)} - k_{x2}\ddot{\bar{x}} - k_{x1}\dot{\bar{x}} - k_{x0}\bar{x} \\ \bar{e}_y &= -k_{y3}\bar{y}^{(3)} - k_{y2}\ddot{\bar{y}} - k_{y1}\dot{\bar{y}} - k_{y0}\bar{y} \\ \bar{e}_z &= -k_{z1}\dot{\bar{z}} - k_{z0}\bar{z} \end{aligned} \tag{10}$$

where the parameters k_{ij}'s are chosen such that the equations $s^2 + k_{i1}s + k_{i0} = 0$, $(i \in \{\eta, \theta, \psi, z\})$ and $s^4 + k_{i3}s^3 + k_{i2}s^2 + k_{i1}s + k_{i0}s = 0$, $(i \in \{x, y\})$ are Hurwitz.

To stabilize the hovering flight mode, at the end of each wingbeat, neglecting the coupling between the torques and the mean vertical thrust $\bar{F}_v$ by approximating it by its average value at $150\,Hz$, the desired wing kinematic parameters for the next wingbeat are calculated as:

$$\begin{aligned} \gamma &= \hat{g}_1(k_1\bar{e}_\eta + k_2\bar{e}_y) \\ \alpha_l &= \hat{g}_2(k_3\bar{e}_\theta + k_4\bar{e}_x, \bar{e}_\psi) \\ \alpha_r &= \hat{g}_3(k_3\bar{e}_\theta + k_4\bar{e}_x, \bar{e}_\psi) \end{aligned} \tag{11}$$

where k_i's indicate the weights on the angular and position errors. Since the approximated linear dynamics assumes small orientation angles, more weight is put on the angular errors in order to stabilize the attitude around the equilibrium point, and at the same time regulate the position. The wing flapping frequency is chosen according to $150 + 10 \times sign(\bar{e}_z)$, where the function $sign(s)$ returns 1 if s is positive and -1 otherwise.

6 Simulation Results

The proposed control method is simulated with VIFS [9] for a continuous 200 wingbeats and Figure 8,9, and 10 show the resulting position and velocity trajectories, together with the corresponding parameters chosen at each wingbeat. The linear and angular displacements are recovered from $[15\,40\,-20]$ millimeters and $[30^o\,-45^o\,60^o]$ to its equilibrium point within 600 milliseconds in less than 90 wingbeats. It shows that the controller succeeds in stabilizing hovering and control both position and attitude. Moreover, the MFI shows a chattering motion about the equilibrium position. This phenomenon is mainly due to the periodic motion of the flapping wing, and also due to the fact that nonlinearity and coupling among dynamic variables have been neglected.

7 Conclusion

In this work, we have parameterized the wing kinematics by a small set of parameters to decouple the control of the average torques generated by the wings. Based on the inverse map of the parameter and mean torques,

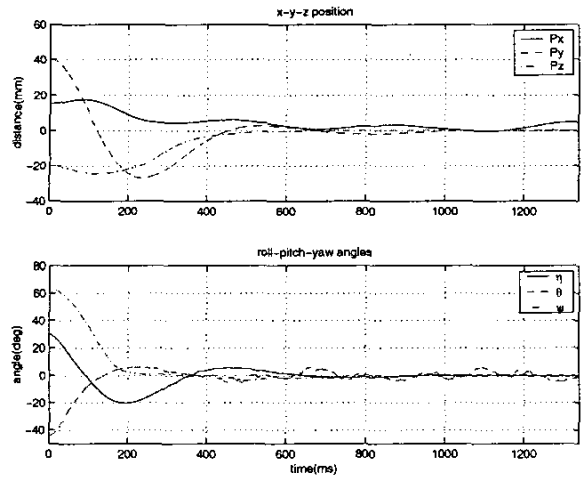

Figure 8: MFI position and orientation trajectories.

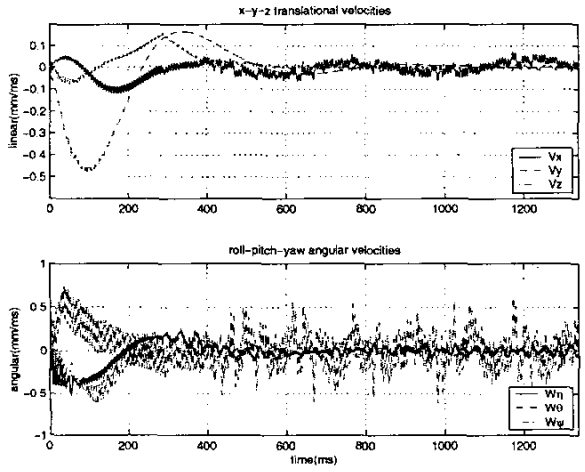

Figure 9: MFI linear and angular velocities.

a controller was designed which schedules the desired wing kinematic parameters based on the feedback error at the end of each wingbeat. Based on the linearized dynamics under the small angle assumption, the controller succeeds in regulating MFI's attitude and therefore control its position.

In order to simplify the model, we do not take into account external disturbances such as wind gust and rain. However, our goal is to design a controller with a large basin of stability, such that the MFI is able to recover the hovering flight mode even from an upside-down position. As a consequence, albeit wind gust and rain may degrade flight performance, they should not compromise the overall behavior of the MFI. We will address this issue in future work. Another major assumption was the full access to the insect states. In practice, perfect state information is not available. However, the MFI will be equipped with various sensors such as gyroscopes, flow sensors and light detectors. Therefore

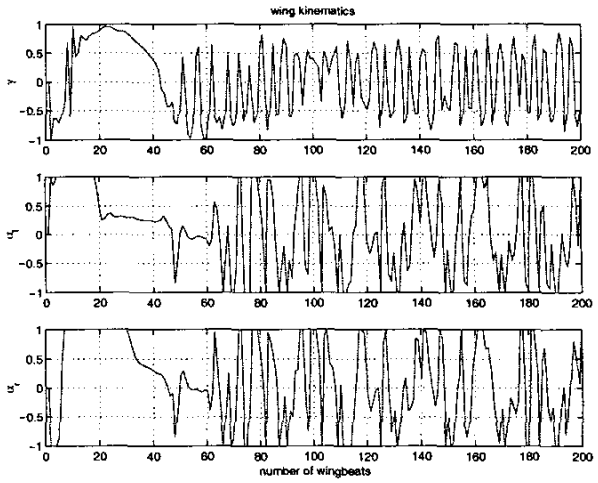

Figure 10: Parameters chosen at each wingbeat.

future work will also address sensor modeling and output feedback.

References

[1] D. H. Shim, H. J. Kim, and S.S. Sastry, "Control system design for rotorcraft-based unmanned aerial vehicles using time-domain system identification," in *Proc. of the IEEE Int. Conf. on Control Applications*, Anchorage, 2000.

[2] T. J. Koo and S. Sastry, "Output tracking control design of a helicopter model based on approximate linearization," in *Proc. of the IEEE Conf. on Decision and Control*, 1998.

[3] R.S. Fearing, K.H. Chiang, M.H. Dickinson, D.L. Pick, M. Sitti, and J. Yan, "Transmission mechanism for a Micromechanical Flying Insect," in *Proc. of the IEEE Int. Conf. on Robotics and Automation*, San Francisco, USA, Apr. 2000, pp. 1509–1515.

[4] M. Sitti, "PZT actuaoted four-bar mechanism with two flexible links for micromechanical flying insect thorax," in *Proc. of the IEEE Int. Conf. on Robotics and Automation*, Korea, 2001 (to appear).

[5] L. Schenato, X. Deng, and S.S. Sastry, "Flight control system for a micromechanical flying insect," in *Proc. of the IEEE Int. Conf. on Robotics and Automation*, Korea, 2001 (to appear).

[6] S.S. Sastry, *Nonlinear Systems: Analysis, Stability, and Control*, Springer Verlag, 1999.

[7] R. Sanchez-Pena and M. Sznaier, *Robust Systems: Theory and Applications*, Wiley, 1998.

[8] M.H. Dickinson, F.O. Lehnmann, and S.S. Sane, "Wing rotation and the aerodynamic basis of insect flight," *Science*, vol. 284, no. 5422, pp. 1954–1960, 1999.

[9] L. Schenato, X. Deng, W.C. Wu, and S.S. Sastry, "Virtual insect flight simulator (vifs): A software testbed for insect flight," in *Proc. of the IEEE Int. Conf. on Robotics and Automation*, Korea, 2001 (to appear).

[10] R. M. Murray, Z. Li, and S.S. Sastry, *A Mathematical Introduction to Robotic Manipulation*, CRC Press, 1994.